Journal of
Synchrotron
Radiation

ISSN 0909-0495

Received 23 July 2011
Accepted 30 December 2011

In vivo physiological saline-infused hepatic vessel imaging using a two-crystal-interferometer-based phase-contrast X-ray technique

Tohoru Takeda,[a,b]* Akio Yoneyama,[c] Jin Wu,[b,d] Thet-Thet-Lwin,[a,b] Atsushi Momose[e] and Kazuyuki Hyodo[f]

[a]Allied Health Sciences and Graduate School of Medical Science, Kitasato University, 1-15-1 Kitasato, Minami-ku, Sagamihara, Kanagawa 252-0373, Japan, [b]Institute of Clinical Medicine, University of Tsukuba, Tsukuba-shi, Ibaraki 305-8575, Japan, [c]Advanced Research Laboratory, Hitachi Ltd, Hatoyama, Saitama 350-0395, Japan, [d]Division of Clinical Neuroscience, Chiba University Center for Forensic Mental Health, 1-8-1 Inohana, Chiba 260-8670, Japan, [e]Department of Advanced Materials Science, Graduate School of Frontier Sciences, The University of Tokyo, 5-1-5 Kashiwanoha, Kashiwa-shi, Chiba 277-8561, Japan, and [f]High Energy Accelerator Research Organization, Tsukuba-shi, Ibaraki 305-0801, Japan. E-mail: t.takeda@kitasato-u.ac.jp

Using a two-crystal-interferometer-based phase-contrast X-ray imaging system, the portal vein, capillary vessel area and hepatic vein of live rats were revealed sequentially by injecting physiological saline *via* the portal vein. Vessels greater than 0.06 mm in diameter were clearly shown with low levels of X-rays (552 μGy). This suggests that *in vivo* vessel imaging of small animals can be performed as conventional angiography without the side effects of the presently used iodine contrast agents.

Keywords: *in vivo* hepatic vessel imaging; two-crystal interferometer; phase-contrast X-ray technique; physiological saline.

1. Introduction

Vessel imaging plays a vital role in the diagnosis of stenosis, obstruction and collateral formation in coronary arteries and cerebral arteries, vessel structures of various organs and neovascularity in tumors. Conventional X-ray angiography using the absorption-contrast phenomenon is widely used to demonstrate vessel structures. Since the difference in the X-ray absorption of the blood against surrounding tissues is very small, the use of an iodine contrast agent composed of triiodobenzoic acid derivatives is indispensable in vessel imaging. However, an iodine contrast agent with various demerits, such as high viscosity, high osmolarity and allergenicity, causes adverse reactions ranging from minor to severe, sometimes resulting in death (Katayama *et al.*, 1990).

In contrast, the phase-contrast X-ray technique that detects minute changes of density has about 1000-fold greater sensitivity than absorption for low-atomic-number elements such as hydrogen, carbon, nitrogen and oxygen (Momose & Fukuda, 1995; Momose, 1995; Takeda *et al.*, 1995). Several phase-contrast X-ray imaging techniques (Fitzgerald, 2000; Momose, 2005) such as the Bonse–Hart-type crystal X-ray interferometer-based technique (Bonse & Hart, 1965), the refraction-based technique using crystal diffraction (diffraction-enhanced imaging) (Davis *et al.*, 1995; Ingal & Beliaevskaya, 1995; Chapman *et al.*, 1997; Arfelli *et al.*, 2000; Pisano *et al.*, 2000), the propagation-based technique (Snigirev *et al.*, 1995; Wilkins *et al.*, 1996; Yagi *et al.*, 1999; Hwu *et al.*, 1999) and the grating (Talbot) interferometer technique (Momose *et al.*, 2003; Weitkamp *et al.*, 2005; Pfeiffer *et al.*, 2006) have been developed. Among these methods an interferometer-based method using a crystal X-ray interferometer is the most sensitive method for detecting minute differences of density (Fitzgerald, 2000; Yoneyama *et al.*, 2008). Detailed inner structures of soft tissue that could not be revealed by the absorption-contrast X-ray technique were clearly depicted in phase maps of rat cerebellum (Momose & Fukuda, 1995) and human metastatic liver tumor (Takeda *et al.*, 1995), and phase-contrast X-ray CT images of rabbit cancer (Momose *et al.*, 1996), rat brain (Bonse & Busch, 1996; Beckmann *et al.*, 1997) and human cancer (Takeda *et al.*, 2000) using a monolithic X-ray interferometer.

In phase-contrast X-ray imaging, images of vessels can be generated to detect the minute density difference against the surrounding vessel wall, so the image contrast is obtained by the use of only physiological saline. Our previous study demonstrated that *ex vivo* phase-contrast X-ray imaging with a monolithic interferometer enabled clear depiction of the hepatic vessels using physiological saline as a contrast agent (Takeda *et al.*, 2002). In the monolithic X-ray interferometer-based imaging system, the distance between the object and the half-mirror was less than 2 cm owing to the limited geometrical structure of the monolithic X-ray interferometer (Takeda & Itai, 2001; Takeda *et al.*, 2009). As such, the heat

effects from the live object disturbed the recording of phase-contrast X-ray images because the object was set near the half-mirror during the data acquisition, and the half-mirror of the interferometer could not be stabilized at the ångström order by heat.

A two-crystal X-ray interferometer-based imaging system enables reduction of the heat effects of a living object by extending the geometrical distance between the object and the half-mirror to more than 15 cm. Here, using this phase-contrast X-ray imaging system, *in vivo* hepatic vessel imaging is reported for the first time using physiological saline as a contrast agent.

2. Methods

2.1. Phase-contrast X-ray imaging system

The phase-contrast X-ray imaging system (Yoneyama *et al.*, 2004) consisted of a Si (220) asymmetric-cut crystal for forming a two-dimensional beam, a two-crystal X-ray interferometer, a phase shifter, an object cell and an X-ray CCD camera (Fig. 1). The two-crystal X-ray interferometer was made using a commercially available 10 cm-diameter highly perfect single-crystal silicon ingot. The pixel size of the X-ray CCD camera was 0.018 mm × 0.018 mm with 2048 × 2048 pixels, and a dynamic range of 14 bits. The experiment was performed at the Photon Factory synchrotron X-ray source in Tsukuba, Japan. The X-ray energy was set at 17.7 keV and the X-ray flux in front of the sample cell was 184 μGy s^{-1} at a beam current of 430 mA with 2.5 GeV energy.

2.2. Phase map

The spatial distribution of the phase shift caused by a sample was depicted using the Fourier technique because this technique (Takeda *et al.*, 1982) can acquire the image data five-fold faster than the conventionally used interferometric technique (Momose & Fukuda, 1995). A phase map of the object was acquired by a 3 s exposure. Data transfer from the CCD camera to a computer required 1.8 s, so the time interval of each image became 4.8 s. The rat liver was imaged in a cell filled with physiological saline to reduce the variation of the object thickness. The thickness of the cell was 12 mm and the total X-ray exposure was 552 μGy $frame^{-1}$.

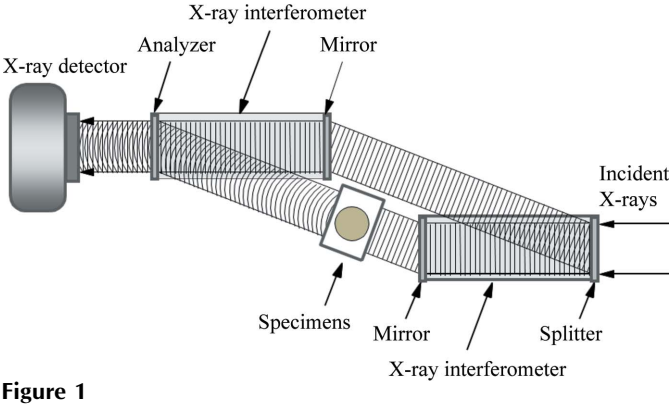

Figure 1
Schematic diagram of the two-crystal-interferometer-based phase-contrast X-ray imaging system.

2.3. Selection of contrast agent

Since, in phase-contrast X-ray imaging, low-atomic-number elements cause a sufficient phase shift, contrast agents not containing heavy elements such as iodine were investigated. Physiological saline had the highest contrast enhancement, and enabled clear imaging of the vessels in the excised liver of rats, so it was selected for use as the contrast agent of the vessels (Takeda *et al.*, 2002).

2.4. Animal preparation

Five Wistar rats were anesthetized using pentobarbital. A 25-gauge catheter was surgically inserted into the portal vein and was ligated by silk thread. Then, a part of the hepatic lobes is bent and protruded from the abdomen in order to take a projection image of the liver. 2 ml of physiological saline was injected using an injector at a rate of 0.1 ml s^{-1} (M-800C, Nemoto-Kyorindo, Tokyo, Japan). The present experiment was approved by the Medical Committee for the Use of Animals in Research of the University of Tsukuba, and conformed to the guidelines of the American Physiological Society.

3. Results

Hepatic vessels of rat injected with physiological saline *via* the portal vein clearly showed up as dark grey areas in the phase map (Fig. 2), since physiological saline has a low refractive index compared with normal vessel walls and liver tissue. The phase map showed the portal vein, capillary vessel area and hepatic vein sequentially. A hepatic vessel of about 0.06 mm in diameter was clearly shown.

One rat showed obstruction of the distal portal branch, and a perfusion defect was revealed in the region of the obstructed vessel at the capillary phase (Fig. 3). In another rat, a catheter was inserted into a deep portion of the portal vein, and selective angiography of the portal vein, named super-selective catheterization, was carried out. The super-selected portal branch was revealed on the right-hand side of the hepatic lobe; however, the left-hand side of the hepatic lobe was not shown at all owing to the lack of injection of physiological saline (Fig. 4).

In addition, the time density curve of the hepatic vessel shown in Fig. 2 indicated that the peak times for the portal vein, capillary vessel area and hepatic vein were about 4.8 s, 19.2 s and 28.8 s, respectively, and enabled an estimation of the flow speed (Fig. 5).

4. Discussion

In vivo hepatic vessels of rats could be clearly visualized by the two-crystal phase-contrast X-ray imaging system using physiological saline as a contrast agent. Owing to the lower specific gravity of physiological saline, the high difference in

refractive index between physiological saline and the surrounding soft tissues caused a high contrast in saline-infused vessels. Flow dynamics from the portal vein phase, capillary phase and venous phase were shown sequentially. A hepatic vessel of about 0.06 mm in diameter was shown well. Obstruction of the distal portal branch and a related perfusion defect were also visualized. In addition, the super-selective angiographic procedure also allowed selected vessel imaging as with typical angiography using a conventional iodine contrast agent. Furthermore, quantitative analysis enabled measurement of the density changes of the portal vein, capillary vessel area and hepatic vein. Thus, the phase-contrast X-ray imaging technique allows visualization of the *in vivo* vessel as with conventional angiography, but using only physiological saline.

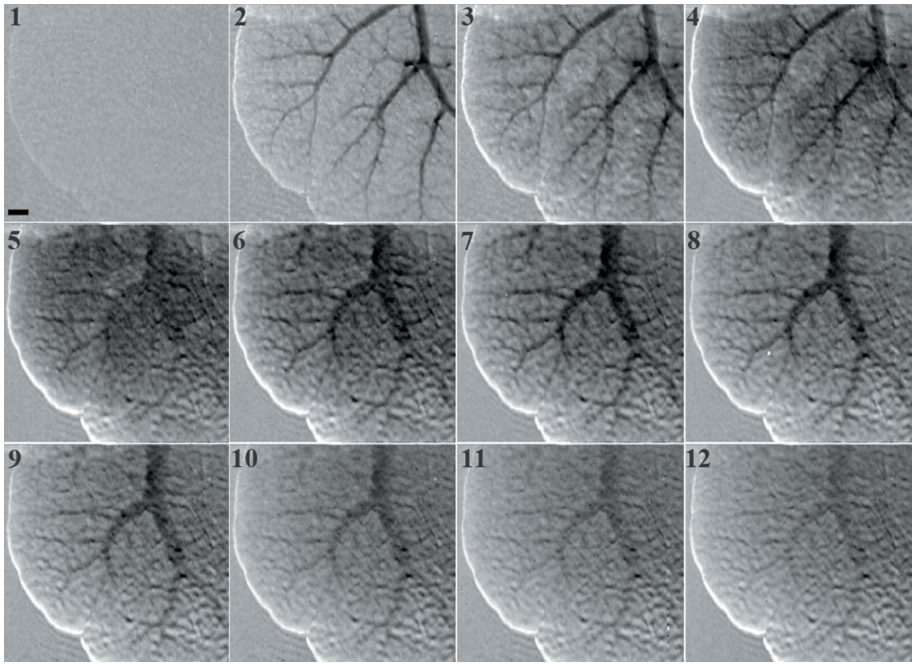

Figure 2
Hepatic vessels injected with physiological saline *via* the portal vein are clearly shown as dark grey areas in the phase map. The phase map dynamically demonstrated the portal vein, capillary vessel area and hepatic vein sequentially. Frame 1: pre-injection; frames 2 to 4: portal phase; frame 5: capillary phase; frames 6 to 12: hepatic vein phase. Scale bar = 1 mm.

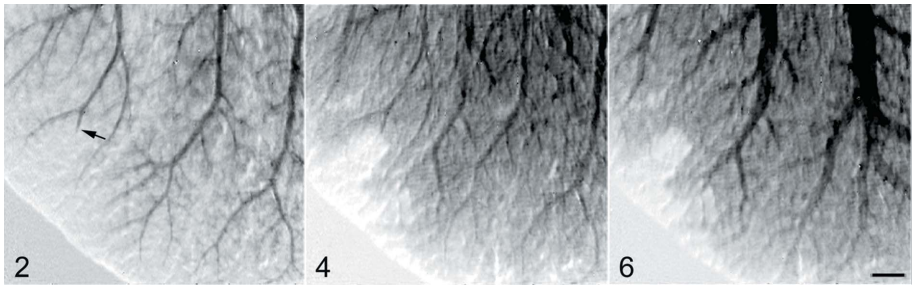

Figure 3
Obstruction of a distal portal branch (black arrow) and a perfusion defect were revealed in the region of an obstructed vessel at the capillary phase. Scale bar = 1 mm.

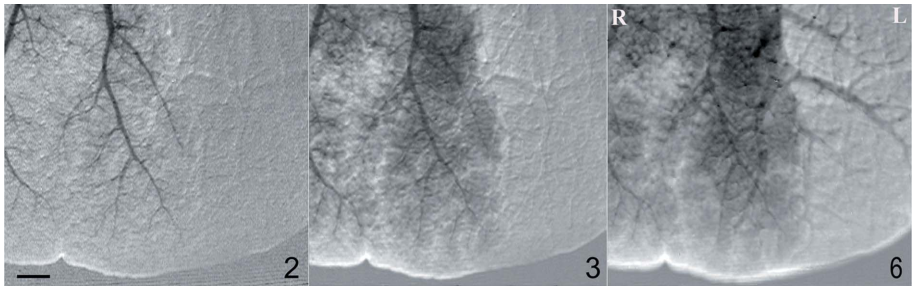

Figure 4
Super-selective angiography of the portal vein with a catheter inserted into a deep portion of the portal vein. The selected portal branch was revealed in the right-hand side of the hepatic lobe, whereas a non-selected hepatic vessel of the left-hand side of the hepatic lobe was not demonstrated in frames 2, 3 and 6. Scale bar = 1 mm. R and L mean right and left side, respectively.

To resolve the small difference in the X-ray absorption of the blood against that of the vessel wall and surrounding tissue, the vessel structure must be imaged by filling the vessel with a contrast agent containing a heavy element such as iodine. However, in such angiographic techniques, unpleasant side effects occur when using iodine contrast agent, such as those owing to high osmolarity, high viscosity and iodine allergenicity (Katayama *et al.*, 1990). Physiological saline composed of sodium chloride without iodine has excellent merits for vessel imaging because the osmolarity and viscosity are reduced by one-half to one-third and one-thirteenth to one-quarter, respectively, compared with iodine contrast agent.

In this phase-contrast technique a vessel of about 0.06 mm in diameter was visualized using an X-ray dose of 552 μGy frame^{-1}. However, in an absorption-contrast method using the iodine contrast agent, the X-ray dose is estimated to be approximately 41-fold greater for depiction of the same vessel diameter. A small amount of radiation exposure to the object will reduce the risk of harm and has excellent benefits for examination.

Thus, the *in vivo* phase-contrast X-ray imaging technique enables the imaging of vessels without the use of iodine contrast agent and with low X-ray dose, and might be applied to assess various vascular diseases, neovascularity of tumors and angiogenesis in the near future.

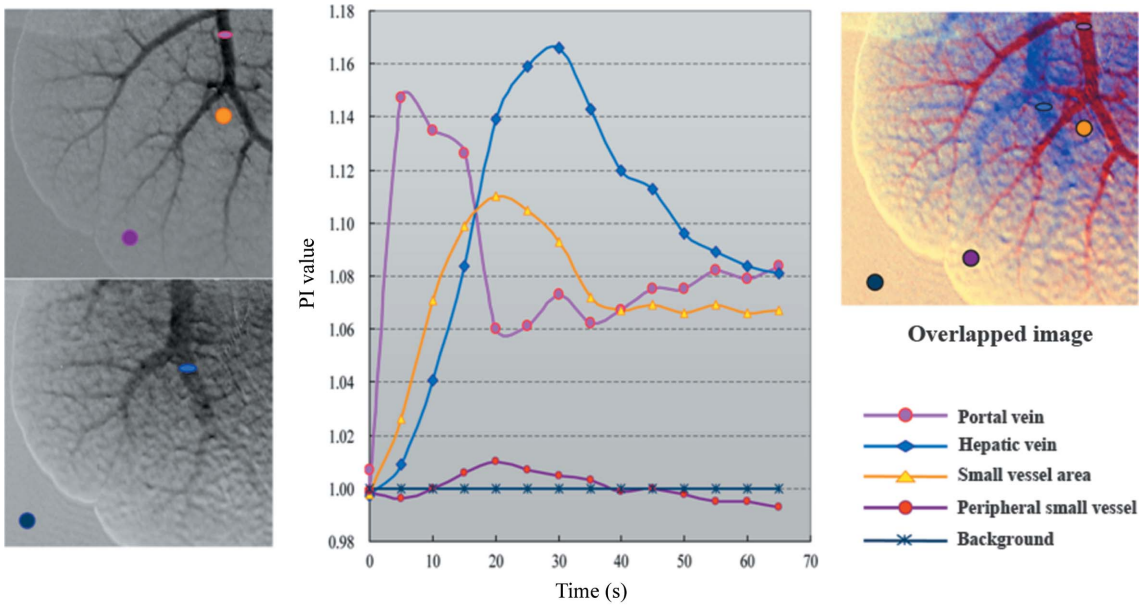

Figure 5
The time density curve of hepatic blood flow. The transit of physiological saline is clearly shown from the portal vein to the hepatic vein. The peak times of the portal vein, capillary area and hepatic vein were about 4.8 s, 19.2 s and 28.8 s, respectively. The overlapped image of the portal phase and venous phase helps to demonstrate the anatomical position of the portal vein and hepatic vein exactly. PI value means the difference in refractive index between vessel and surrounding liver + refractive index of physiological saline normalized as 1.00 in the background.

4.1. Present limitations

In this experiment the time interval for each image must be set to 4.8 s owing to the low sensitivity of the lens-coupled X-ray CCD camera and the long transfer time of the analog-to-digital converter (ADC). Therefore, the data acquisition speed is insufficient for imaging of the vessel and analysis of the detailed flow dynamics. In addition, the visualized vessel diameter was limited to about 0.06 mm. If a fibre-coupled-type X-ray CCD camera and high-speed ADC could be used, the light in front of the CCD camera could be increased by about five-fold, and the data transfer time could be shortened to less than 0.2 s; then one image would be obtained in less than 1 s, and clear *in vivo* images with less blurring would be acquired. Furthermore, an increment of the X-ray flux could enable a shortening of the image acquisition time and the blood flow might be revealed at a rate sufficient for video-imaging.

The present system with small interferometer size has been limited to use in clinical applications, and is applicable for small-animal experiments. However, further developments to widen the view size of the interferometer system may allow clinical applications in the future.

5. Conclusion

Using a two-crystal phase-contrast X-ray imaging system, *in vivo* hepatic vessel imaging under a small X-ray dose was successful using physiological saline without contrast agents containing heavy elements such as iodine.

This research was supported by Special Coordination Funds from the Ministry of Education, Culture, Sports, Science and Technology, and was performed under proposal numbers 2002S2-001 and 2005S2-001, approved by the High Energy Accelerator Research Organization. We are grateful to Mr Kouzou Kobayashi for preparation of the experimental apparatus.

References

Arfelli, F. *et al.* (2000). *Radiology*, **215**, 286–293.
Beckmann, F., Bonse, U., Busch, F. & Günnewig, O. (1997). *J. Comput. Assist. Tomogr.* **21**, 539–553.
Bonse, U. & Busch, F. (1996). *Prog. Biophys. Mol. Biol.* **65**, 133–169.
Bonse, U. & Hart, M. (1965). *Appl. Phys. Lett.* **6**, 155–156.
Chapman, D., Thomlinson, W., Johnston, R. E., Washburn, D., Pisano, E., Gmür, N., Zhong, Z., Menk, R., Arfelli, F. & Sayers, D. (1997). *Phys. Med. Biol.* **42**, 2015–2025.
Davis, T. J., Gao, D., Gureyev, T. E., Stevenson, A. W. & Wilkins, S. W. (1995). *Nature (London)*, **373**, 595–598.
Fitzgerald, R. (2000). *Phys. Today*, **53**, 23–28.
Hwu, Y., Hsieh, H., Lu, M. J., Tsai, W. L., Lin, H. M., Goh, W. C., Lai, B., Je, J. H., Kim, C. K., Noh, D. Y., Youn, H. S., Tromba, G. & Margaritondo, G. (1999). *J. Appl. Phys.* **86**, 4613–4618.
Ingal, V. N. & Beliaevskaya, E. A. (1995). *J. Phys. D*, **28**, 2314–2317.
Katayama, H., Yamaguchi, K., Kozuka, T., Takashima, T., Seez, P. & Matsuura, K. (1990). *Radiology*, **175**, 621–628.
Momose, A. (1995). *Nucl. Instrum. Methods Phys. Res. A*, **352**, 622–628.
Momose, A. (2005). *Jpn. J. Appl. Phys.* **44**, 6355–6367.
Momose, A. & Fukuda, J. (1995). *Med. Phys.* **22**, 375–379.
Momose, A., Kawamoto, S., Koyama, I., Hamaishi, Y., Takai, K. & Suzuki, Y. (2003). *Jpn. J. Appl. Phys.* **42**, L866–L868.
Momose, A., Takeda, T., Itai, Y. & Hirano, K. (1996). *Nat. Med.* **2**, 473–475.
Pfeiffer, F., Weitkamp, T., Bunk, O. & David, C. (2006). *Nat. Phys.* **2**, 258–261.
Pisano, E. D., Johnston, R. E., Chapman, D., Geradts, J., Iacocca, M. V., Livasy, C. A., Washburn, D. B., Sayers, D. E., Zhong, Z., Kiss, M. Z. & Thomlinson, W. C. (2000). *Radiology*, **214**, 895–901.
Snigirev, A., Snigireva, I., Kohn, V., Kuznetsov, S. & Schelokov, I. (1995). *Rev. Sci. Instrum.* **66**, 5486–5492.
Takeda, M., Ina, H. & Kobayashi, S. (1982). *J. Opt. Soc. Am.* **72**, 156–160.

Takeda, T. & Itai, Y. (2001). *Progress in Pathology*, edited by N. Kirkham and N. R. Lemoine, pp. 81–102. London: Greenwich Medical Media.
Takeda, T., Momose, A., Hirano, K., Haraoka, S., Watanabe, T. & Itai, Y. (2000). *Radiology*, **214**, 298–301.
Takeda, T., Momose, A., Itai, Y., Wu, J. & Hirano, K. (1995). *Acad. Radiol.* **2**, 799–803.
Takeda, T., Momose, A., Wu, J., Yu, Q., Zeniya, T., Thet-Thet-Lwin, Yoneyama, A. & Itai, Y. (2002). *Circulation*, **105**, 1708–1712.
Takeda, T., Yoneyama, A., Takeya, S., Thet-Thet-Lwin & Wu, J. (2009). *Handbook of Interferometers*, edited by D. Halsey and W. Raynor, pp. 288–316. New York: Nova Science.
Weitkamp, T., Diaz, A., David, C., Pfeiffer, F., Stampanoni, M., Cloetens, P. & Ziegler, E. (2005). *Opt. Express*, **13**, 6296–6304.
Wilkins, S. W., Gureyev, T. E., Gao, D., Pogany, A. & Stevenson, A. W. (1996). *Nature (London)*, **384**, 335–338.
Yagi, N., Suzuki, Y., Umetani, K., Kohmura, Y. & Yamasaki, K. (1999). *Med. Phys.* **26**, 2190–2193.
Yoneyama, A., Takeda, T., Tsuchiya, Y., Wu, J., Thet-Thet-Lwin, Koizumi, A., Hyodo, K. & Itai, Y. (2004). *Nucl. Instrum. Methods Phys. Res. A*, **523**, 217–222.
Yoneyama, A., Wu, J., Hyodo, K. & Takeda, T. (2008). *Med. Phys.* **35**, 4724–4734.